Journal of Chromatography, 546 (1991) 159–173
Elsevier Science Publishers B.V., Amsterdam

CHROMSYMP. 2205

Electrodialytic eluent generation and suppression

Ultralow background conductance suppressed anion chromatography

DOUGLAS L. STRONG, CHANG UNG JOUNG[a] and PURNENDU K. DASGUPTA*
Department of Chemistry and Biochemistry, Texas Tech University, Lubbock, TX 79409-1061 (U.S.A.)

ABSTRACT

An electrodialytic generator has been linked to a newly designed electrodialytic suppressor. This combination greatly reduces suppressed conductivity due to residual acids originating from the anionic impurities in the eluent sodium hydroxide and completely eliminates the conductivity contribution from chemical regenerant penetration in the suppressor. The system provides reproducible sodium hydroxide gradients obtained by current programming the generator and is able to operate typically with a suppressed conductivity of 300–400 nS/cm providing commensurate performance with respect to detection limits and response linearity.

INTRODUCTION

In the realm of suppressed anion chromatography the two most commonly used eluents, carbonate and hydroxide, exhibit suppressed conductivities of 12–15 and 2–5 μS/cm, respectively, at typical eluent strengths. For carbonate eluents it is well recognized that the residual conductivity after suppression is largely due to dissociation of the carbonic acid formed in the suppressor. Actually, carbonic acid is also the principal contributor to the suppressed conductance of an hydroxide eluent because carbonate is by far the principal impurity typically present in the stock hydroxide solutions used for dilution. In our experience, the carbonate content of commercial 50% sodium hydroxide solutions ranges from 0.06 to 0.17 mol%. With both eluents, there are also contributions from impurity anions such as Cl^- and SO_4^{2-} which form the corresponding strong acids in the suppressor. Presently, an acid-regenerated membrane device is most commonly used for the continuous ion-exchange process referred to as suppression. With such devices, the penetration of the acid regenerant anion, *e.g.* sulfate, into the suppressor effluent also contributes to the background conductance. A suppressor column packed with ion-exchange resin does

[a] Permanent address: Department of Chemistry, Soonchunhyang University, Onyang, Chungnam 336-600, South Korea.

0021-9673/91/$03.50

not suffer from regenerant penetration but has myriad other, unattractive, characteristics [1] such that its resurrection is hardly likely.

As in most detection systems, it is logical to seek the lowest detector background (which in the present case is the suppressed conductance of the eluent) because a low background is conducive to low noise and hence better limits of detection. In ion chromatography (IC), particularly strong incentives exist to produce essentially a pure solvent background to carry out the ion replacement detection technique [2–7] which can, in principle, be exquisitely sensitive. Further, coupling the column effluent to a mass spectrometer [8] is facilitated when the effluent is free of dissolved solids. For an acid-regenerated membrane suppressor, regenerant penetration can be reduced by using an acid with a large and preferably multiply charged counterion, the bulk and the charge of this Donnan-forbidden ion deters transmembrane transport due to a lower diffusion coefficient and better electrostatic exclusion. Thus, the use of acids such as poly(styrenesulfonic), naphthalenetrisulfonic, dodecylbenzenesulfonic acid, etc. has been advocated for this purpose [9–13]. It is possible to avoid renegerant penetration altogether by electrodialytically removing the eluent cation. The necessary H^+ ions are generated by the electrolysis of water. Although a number of papers and patents exist on the electrodialytic scheme [14–17], all but one [17] use acid electrolytes and it is questionable with the others as to how much of the suppression process is actually accomplished electrodialytically. It has in fact been shown that applying an electric field in an otherwise functional acid-regenerated membrane suppressor is not necessarily beneficial [17].

With an electrodialytic suppressor (EDS) that can function adequately without any acid electrolyte, the only remaining obstacle to the attainment of a detector background approaching that of pure water with a suppressed hydroxide eluent is anionic impurities in the eluent. We have previously reported on the construction and characteristics of a series of on-line electrodialytic sodium hydroxide generators (EDGs) based on perfluorosulfonate cation exchange (catex) membranes [18,19]. These generators produce ultrapure sodium hydroxide on-line and afford the added versatility of gradient elution with isocratic pumps because the output concentration from the generator varies directly with the current input which can be programmed.

The full advantage of the purity of an electrodialytically generated eluent can only be realized when it is used in conjunction with an EDS. The characteristics of such a system are reported here.

EXPERIMENTAL

Materials

Stock sodium hydroxide solution was 50% sodium hydroxide (J. T. Baker). House-distilled water fed a Barnstead Nanopure unit, the output of this was used as the feed for a continuously recirculating water polisher (Dionex). The eluent generators were supplied off a tee in the recirculating loop.

Chromatographic system

EDGs. Two different styles of EDG devices were used in this work. The operating principles of these are illustrated in Fig. 1. In one (Fig. 1a), a single tubular Nafion membrane (811x, Perma-pure Products, Toms River, NJ, U.S.A.) containing

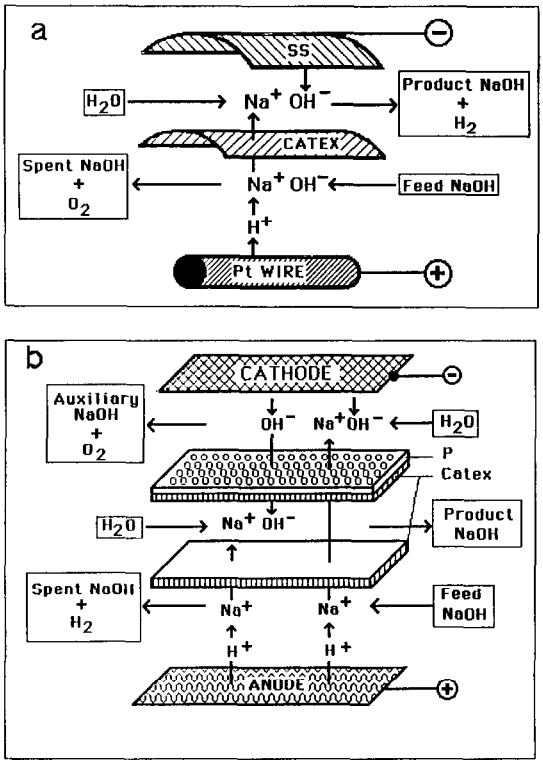

Fig. 1. Principles of operation for (a) a single membrane tubular and (b) a double membrane/perforated plate (P) planar electrodialytic sodium hydroxide generator.

an inserted platinum wire and surrounded by a stainless steel jacket (17 cm × 1 mm I.D.) is fed with ordinary sodium hydroxide in the lumen and sodium hydroxide and hydrogen are produced in the outer channel (type 1 device) [18]. The second device is based on electrodialytic transport through one catex membrane (Nafion 117, Aldrich) and Donnan breakdown of a second similar catex membrane [19] (Fig. 1b). Briefly, the device is built inside a micromembrane suppressor shell (MMS, Dionex). The feed sodium hydroxide flows below one catex membrane and this bottom flow channel contains 50 cm of 0.25 mm diameter platinum wire woven as an electrode on a coarse weave cation-exchange screen (Dionex). Another catex membrane lies atop the first one and the intervening space constitutes the product channel; water is fed from one end and the gas-free product sodium hydroxide flows out of the other end. Atop the top catex membrane is placed a perforated plate P of FEP-Teflon (0.5 mm thick, 4 rows of evenly spaced 1.55 mm holes, 72/row) and water flows over this; atop the plate is placed a stainless-steel screen to function as the cathode. Accumulation of significant concentrations of sodium hydroxide take place in the wells of the plate and causes Donnan breakdown of the top membrane, permitting OH^- transport through it. This (type 2) device generates a gas-free product. Complete construction details of the above devices have been given previously [18,19].

The type 1 EDG output was fed to a degasser made by machining shallow channels into two aligned blocks of nylon separated by a hydrophobic gas-permeable membrane sandwiched in-between. The flow channels were accessed by appropriately drilled holes in the blocks. Microporous Teflon (Gore-Tex, W. L. Gore, Elkton, MD, U.S.A.) or polypropylene (Celgard, Hoechst–Celanese, Charlotte, NC, U.S.A.) are both suitable membrane materials, with the latter being more resistant to stretch induced by the sudden nature of the pump intake strokes. Also, because of the short duration of the intake strokes of a typical piston pump, movement of fluid through the generator product channel is intermittent while the electrical current is constant. A gradient mixer cartridge is therefore placed after the degasser to ameliorate any temporal imhomogeneities in the sodium hydroxide concentration. The degassed output was fed via a tee into the dual inputs of a Dionex Model 4000i pump directly into the pump head. The EDG was under the control of a constant current source, temporally programmable by an AT-class computer. The overall experimental arrangement is depicted in Fig. 2. The type 2 EDG was controlled by a manually adjustable constant current source and its output was fed to a Beckman 110A pump equipped with a pulse dampener. Common to both systems were an injection volume of 50 μl, an AS-5A column, an EDS described below, a CDM-II conductivity detector (Dionex) and a generator product flow of 1 ml/min as controlled by the chromatographic pump. Chromatographic results were acquired on a disk-based C-R3A integrator system (Shimadzu Scientific).

EDS. The EDS used in these experiments is a planar device constructed within a Dionex MMS body. This new design is simpler to fabricate than the previously reported tubular EDS [17] and does not require any carbon packing. The operating principle is illustrated in Fig. 3. An understanding of the fabrication details of the current EDS given below is facilitated by familiarity with the design of the standard MMS devices as described by Stillian [20]. The MMS shell consists of two blocks, one with four external connections (A) and another with no external connections (B). There are three flow channels in the assembled MMS, a central eluent channel flanked by a renegerant channel on each side. In the commercial device, the two flanking channels are connected in parallel and are fed from a common regenerant source. In

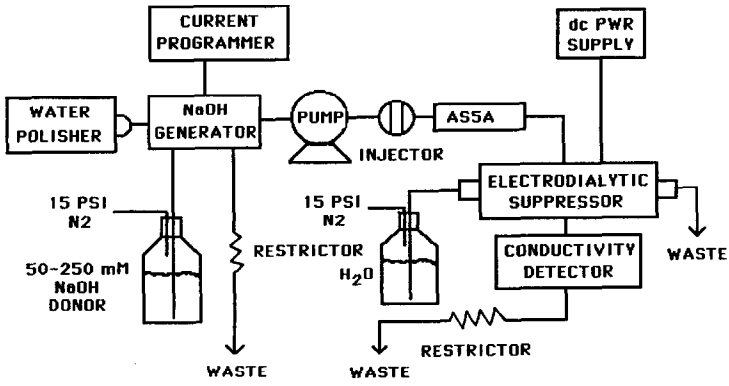

Fig. 2. Complete experimental arrangement including the electrodialytic generator and suppressor.

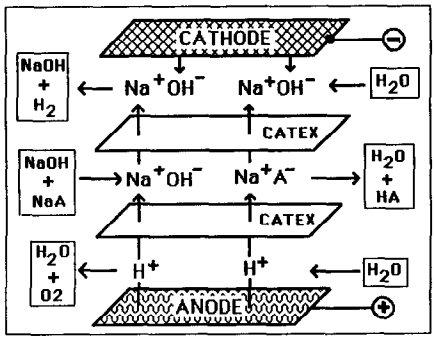

Fig. 3. Principle of operation of the electrodialytic suppressor.

the present device, these flanking channels must be separated for use as the cathode and anode flows of the EDS. This is done by plugging the inter-block connections in the MMS shell and by drilling appropriately placed holes in the side of block B and press-fitting stainless-steel tubing in these holes to access the flow channel in the block. The original regenerant flow connections in block A now access only the flow channel in this block. It is important that block B be selected as the anode channel because the flow path is longer and the effective membrane area greater than in the cathode compartment. Referring to Fig. 3, it can be seen that the anode and the cathode membrane remain respectively in the H^+- and Na^+-form. It is advantageous to have the membrane with the greater length as the H^+-form anode membrane; this diminishes the opportunity for the suppressor effluent to contact a Na^+-laden membrane as it exits.

For the anode, 50 cm of 250 μm diameter platinum wire was woven onto one of the original MMS coarse catex screens and a short length of thick stainless steel wire pressed through a hole drilled through the bottom of block B to contact the platinum wire. For the cathode, a 200 mesh stainless steel screen was cut to fit the well in block A and a parafilm sheet pressed into the screen with a hydraulic press at *ca.* 0.26 ton/in.^{2} to form a gasket on the screen; this closely resembles the parafilm gasket on the ion-exchange screen from this channel in the original MMS device. Like the MMS, the eluent flow channel is accessed through holes in the cathode membrane. Holes are punched in the cathode screen at these locations to keep the cathode out of the eluent flow where it may introduce gas during operation. A polypropylene mesh (250 μm opening, D-CMP-250, Small Parts, Miami, FL, U.S..) separates the cathode from the cathode membrane while a coarse catex screen separates the anode from the anode membrane. Without these, gas appears in the suppressed eluent. Electrical contact to the cathode is established in a fashion similar to that with the anode by a push-fitted stainless-steel rod through a hole in the top of block A. A fine mesh ion-exchange screen is present in the eluent channel of the MMS, a similar catex screen occupies the eluent channel of the present EDS as well. Water flow through the flanking channels and eluent flow through the central channel were all maintained at 1 ml/min.

Measurement of the permeation of carbon dioxide through polymeric tubing

The intrusion of carbon dioxide through polymeric components is a major concern in maintaining the purity of an ultrapure sodium hydroxide eluent. The permeation rate of carbon dioxide through Tefzel tubing was studied in the following manner. The pure water output from the water polisher was first directly connected to the injection port of the chromatographic system with the minimum tubing necessary (4 cm) and a "blank" obtained by allowing the sample loop to flush for 30 s, then injecting. A 2.1-m length of Tefzel tubing (0.5 mm wall, 0.5 mm I.D.) was then inserted between the water polisher and injection port. The valve was next put in the load mode and water flowed through the Tefzel tubing and the sample loop of the valve for $\geqslant$ 1 min. The residence time of the water in the Tefzel conduit was 0.42 min. The sample was then injected and after 9.5 min the analysis cycle was completed, the valve was put in the load mode again for 20 s to analyze the water that remained stationary in the Tefzel conduit during the preceding analytical cycle.

Conductance measurement of sodium hydroxide solutions

The specific conductances of standard sodium hydroxide solutions were measured as a function of concentration (0–100 m*M*) and temperature (15–40°C). A home-made flow-through thermostating device was used for temperature adjustment of the sodium hydroxide solution. Sodium hydroxide solutions of known concentration were pumped at 1 ml/min through *ca.* 35 cm of coiled stainless steel tubing embedded in silver epoxy atop two Peltier heat pumps (30 × 30 × 4 mm, Melcor, Trenton, NJ, U.S.A.) stacked serially above each other. The bottom of the stack was mounted on a fan-cooled finned heat sink with silicone heat sink compound. The temperature of the assembly was measured by a reference current source that produces an output of 1 μA/K (AD-540, Analog Devices, Norwood, MA, U.S.A.) which is used in turn by appropriate control electronics to maintain the temperature within 0.1°C of set temperature. After exiting the thermostating coil the liquid passed sequentially through a Dionex CDM-II detector cell D1 and a home-made detector cell D2 (see below). Minimum lengths of polymeric connecting tubing were used to connect the cells to each other and to the thermostating cell and the whole assembly above the bottom plate of the Peltier stack was insulated with styrofoam.

Cell D2 was constructed to have a significantly larger cell constant than D1. This was necessary to measure the conductivity of sodium hydroxide solutions $\geqslant$ 5 m*M* in concentration because the detector electronics is incapable of measuring conductance values above 1.3 mS. The cell constant of D1 is 1.0 cm^{-1}. Increasing the cell constant proportionately increases the applicable range of measurement. Cell D2 was constructed by securing two 3 cm long × 1/16 in. O.D. thin wall stainless steel tubing segments to each side of a 10–32 poly(etheretherketone) (PEEK) female compression coupling. The steel tubes serve both as the flow conduit and the measuring electrodes. Both cells are connected to the Dionex CDM-II electronics module through a switchbox which allows either cell to be read. The cell constant of D2 was measured to be *ca.* 14 cm^{-1} at 25°C. During conductivity calibrations of sodium hydroxide solutions, the temperature compensation feature of the detector electronics was disabled. During chromatographic use, however, the conductance measured with D2 is temperature-compensated by the thermistor located in the serially connected D1 cell. It is possible to modify the electrode connections to cell D1 itself to greatly increase the

effective cell constant. Using the two original electrodes in common as one electrode and the cell grounding block as the other electrode results in a cell with an effective cell constant of *ca.* 320 cm^{-1}. Cell D2, however, has a very low flow resistance and, when terminated with the proper fittings, it can be used between the pump and the injector at eluent pressures commonly encountered in IC.

Corrections to the CDM readouts are necessary at high conductance values. Made for use in suppressed IC, the detector is optimized for the 0–200 μS range. The necessary correction is very significant at conductance levels above 1 mS. Note that this correction pertains to the apparent conductance values and not to the specific conductance values. Thus with two cells of different cell constants connected in series, it is possible to evaluate the necessary correction factors by noting the ratio of the apparent conductance values read by D1 and D2 under the following conditions: (a) when both read $<$ 200 μS and (b) when the concentration is increased further to explore the full range of the detector readout with cell D1 without exceeding a reading of 200 μS with cell D2. Assuming that the ratio of the cell constants is independent of the measured conductance it is now possible to arrive at the correction factors necessary to correct the detector reading at high conductance readouts. Interpolation through a second degree polynomial fit was used in this work to arrive at the correction factors.

RESULTS AND DISCUSSION

Concentrations of sodium hydroxide by conductance measurements

Should the present method of electrochemical eluent generation eventually enjoy widespread use, it may not be necessary to specify eluent concentrations *per se* to describe a given chromatographic condition. For a faradaically efficient generator, specification of the product flow-rate and current automatically specifies the generated concentration. To characterize generators with less than faradaic efficiency, the actual concentration generated at a given current must be known. An on-line measurement of the generated eluent concentration is also a good diagnostic tool for overall system behavior and is most easily accomplished in the present case with conductance measurements. Measuring such high specific conductance values does not require particularly sophisticated electronics and a dedicated detector can be provided. In general, however, it is not necessary to continuously monitor the eluent concentration during chromatography. The detector cell of a large cell constant to measure the eluent concentration can be simply switch-multiplexed to the chromatographic detector electronics. The results of the conductivity calibrations are shown in Fig. 4a as linear and in Fig. 4b as log–log plots. These data show that a significant deviation from linearity is observed at higher concentrations. Insofar as the temperature dependence is concerned, a comparison of Fig. 4a and b shows that although on an absolute scale the conductivities increasingly diverge from each other at higher concentrations, on a relative scale the conductivities maintain essentially the same relationship as a function of temperature, regardless of the concentration. The nonlinear dependence of the conductance on concentration at any given temperature is satisfactorily represented at each temperature by a quadratic equation and these are presented in Table I. It should be noted that the specific conductance values as reported in this work and as represented by the equations in Table I differ significantly,

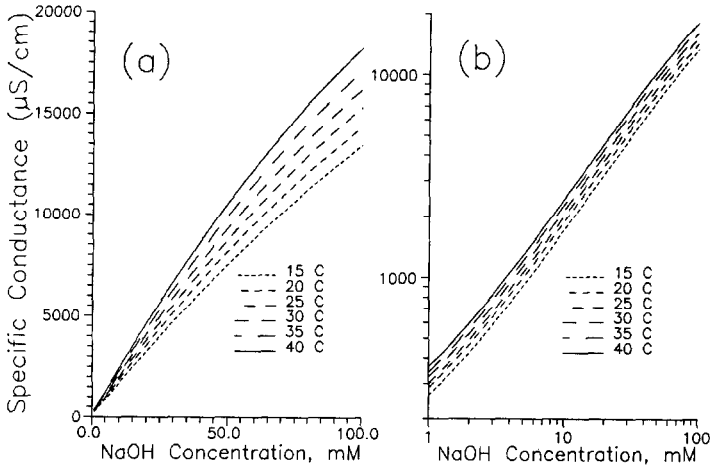

Fig. 4. Specific conductance of sodium hydroxide solutions as a function of temperature and concentration shown in (a) linear and (b) logarithmic plots.

especially at higher concentrations, from conductance values calculable from equivalent conductance data reported for sodium hydroxide solutions at 18°C in standard compilations [21]. Whether this is due to intrinsic differences between conductance measurements in static and flowing situations [22], the presence of impurities or the failure in our case to fully correct for the error in the readout at high conductance values could not be established with certainty. Realistically, a user interested in the absolute accuracy of such calibrations and wishing to use a different conductance detector for this purpose will likely need to perform his own calibrations, given the general inability of chromatographic conductivity detectors to produce reliable values with high conductance solutions. Nevertheless, the temperature-dependence data represent a relative measurement and are expected to be valid, regardless of the absolute accuracy. Fig. 5 shows the specific conductance of sodium hydroxide solutions of different concentrations as a function of temperature. As may be evident, the

TABLE I

COEFFICIENTS OF QUADRATIC EQUATION DESCRIBING SPECIFIC CONDUCTANCE OF NaOH

Specific conductance = $A_0 + A_1$[NaOH, mM] + A_2[NaOH, mM]^2.

Temperature (°C)	Coefficient		
	Zero degree, A_0	First degree, A_1	Second degree, A_2
15	99.4	164.3	−0.3090
20	106.1	181.6	−0.3936
25	106.9	193.9	−0.4179
30	116.8	207.5	−0.4679
35	118.5	222.4	−0.5244
40	126.1	236.3	−0.5533

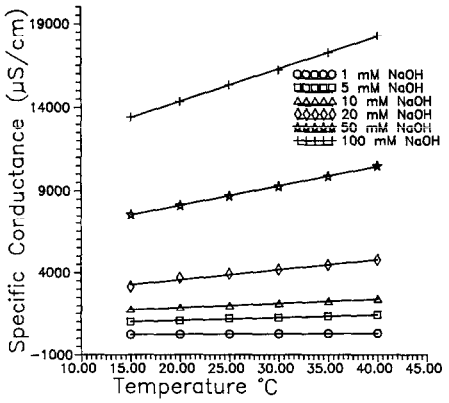

Fig. 5. Specific conductance of sodium hydroxide solutions of individual concentrations as a function of temperature.

data indicate a linear dependence on temperature. Temperature dependence is often expressed as a percent dependence per °C, although such results are clearly dependent on the reference temperature. Referred to 25°C, the data in Fig. 5 represent a temperature dependence of 1.34 ± 0.12%/°C.

The EDGs and EDS: operation and performance. Fig. 6 shows the generated product concentrations and the suppressed product conductances as a function of the generator current. All data were obtained with a feed of 250 m*M* sodium hydroxide flowing at 2 ml/min. The suppressor current was optimized for each generator current, typically requiring 110–120% of the faradaic transport current. For reasons not fully understood, a large excess of suppressor current not only leads to greater baseline noise but the background conductance actually increases as well. Otherwise, as Fig. 6 shows, the background conductance remains 300–400 nS/cm, regardless of the generated eluent concentration. Even when pure water is input to the EDS in place of

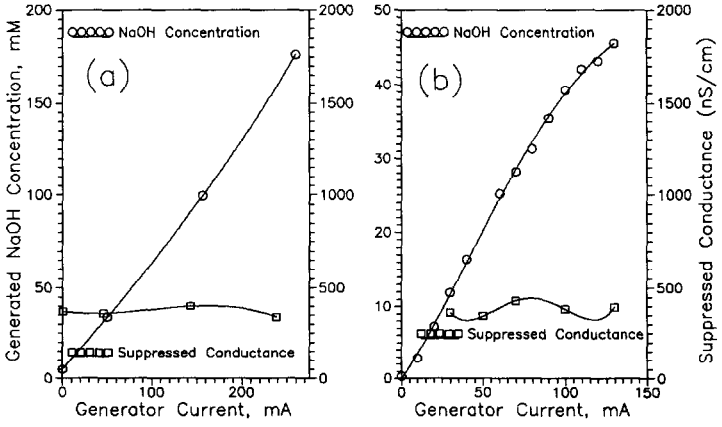

Fig. 6. Generated product concentration as a function of current and the corresponding EDS suppressed conductance for (a) type 1 and (b) type 2 generator. The circles and squares pertain in each case to the left and right ordinate, respectively.

sodium hydroxide, the specific conductance measured by the detector in the presence of a finite amount of current flow (*ca.* 35 mA) is 150–200 nS/cm. Whether this elevation over the theoretical specific conductance of water (*ca.* 60 nS/cm) arises within the suppressor due to electrochemical degradation of some wetted part or results from the permeation of carbon dioxide into the water as it is pumped and transferred to the EDS through Tefzel tubing (see below), is not clear; however, even without any current, the background conductance can not be reduced below *ca.* 100 nS/cm.

The current efficiency of the type 1 generator is excellent; the results shown in Fig. 6a correspond to a linear relationship ($r = 0.999$) with a slope of 0.657 ± 0.024 mM/mA, essentially indistinguishable from the faradaic value of 0.625 mM/mA (at the operative flow-rate of 1 ml/min). With the specific donor concentration used, this device will easily generate 250 mM sodium hydroxide at 1 ml/min. In contrast, the maximum current efficiency of the type 2 device, 0.419 mM/mA, is reached around a current of 60 mA and decreases thereafter. At currents above 100 mA, the product concentration begins to level off. Currents above 130 mA are not practical as gas appears in the product. The 0–260 mA current range in the type 1 device is attained with an applied voltage $\leqslant 3.55$ V while it requires up to 11 V to pass 130 mA through the type 2 device.

The most critical requirement of the overall system appears to be the purity of the water fed to the EDG since, after addition of sodium hydroxide in the generator and its removal in the suppressor, the conductivity of the original water (plus whatever adventitious impurity manages to find its way in) is registered by the detector. The purity of the water which flows as anolyte and catholyte through the EDS is not as critical. Water, originally of resistivity 12 M$\Omega \cdot$ cm, kept in a 4-l polyethylene bottle is adequate even after standing for 2–3 days. The specific recirculating water polisher used exhibits significant pump pulsations and if this is directly connected to the EDS, a baseline noise of related frequency is observed; a pneumatically pressurized water source was therefore preferred. Regarding the feed sodium hydroxide, the donor concentration can be the same as the maximum concentration the generator is expected to deliver but delivered at twice the generated eluent flow-rate. The feed reservoir used in this work was a heavy wall polyethylene container and it was necessary to replace the feed solution every 3–4 days for optimum performance. Apparently within such a period, sufficient carbon dioxide is absorbed through the polyethylene walls to cause an observable rise in the suppressed conductance due to the less than perfect anion rejection by the generator anode membrane. In a similar vein, a donor concentration greater than that necessary compromises the suppressed conductance due to the higher concentration of impurity anions in the donor. Also, with greater donor concentration there is greater zero current penetration of sodium hydroxide through the generator membrane. This means a higher minimum eluent strength with no current applied to the generator. When the donor concentration is reduced to 75 mM, the zero current eluent concentration is *ca.* 0.1 mM sodium hydroxide. All the above factors suggest that the minimum donor concentration be used.

Chromatography

Enhanced sensitivity to carbonate. the first striking feature of this system is its sensitivity for carbonate. Conventional suppressed IC displays relatively poor sensitivity for carbonate; innovative post-column measures were taken by Tanaka and

Fritz [23] to improve the detectability of eluite carbon dioxide in a water eluent ion-exclusion chromatography system. It may be calculated that pure water in equilibrium with atmospheric carbon dioxide contains *ca.* 13 μM total dissolved carbon dioxide. Due to the ubiquity of atmospheric ammonia, the total dissolved carbon dioxide in a water sample exposed to the atmosphere may be somewhat higher. Indeed, even if an aqueous sample is strongly acidic, *ca.* 11 μM carbon dioxide will be dissolved in it at equilibrium. In pure water, a solution of carbon dioxide is *ca.* 11 μM carbon dioxide (aq.) and *ca.* 2 μM each H^+ and HCO_3^-. In suppressed IC many other samples are detectable at these concentrations. Carbonate, however, is normally invisible. With a carbonate eluent, the suppressed product already has *ca.* 5 mM total carbon dioxide species and the addition of 13 μM more to this system has little effect on the equilibrium which is already shifted greatly toward the associated and non-conductive carbon dioxide (aq.). With a 30-mM hydroxide eluent prepared from 50% sodium hydroxide stock containing 0.17 mol% carbon dioxide, there is minimally 50 μM carbonate, not counting the carbon dioxide contribution of the diluent water. The dissociation of the carbonic acid produced from this source seriously masks the response to any carbon dioxide present in the sample. In the present system, the carbon dioxide content of the eluent is minimally 30-fold lower than that of a typical hydroxide eluent system [18] and small amounts of carbonate/dissolved carbon dioxide in a sample should be much more easily detected.

The great sensitivity of the system to carbon dioxide is a mixed blessing. In ultratrace analysis, carbon dioxide will invariably show up as a major peak. This is illustrated in the chromatogram of Fig. 7. At concentrations of analyte ions of interest below *ca.* 1 μM, unless chromatographic conditions are carefully chosen, a large carbonate peak can significantly overlap the nitrate peak.

Permeation of carbon dioxide through tubing. The permeation of carbon dioxide through Tefzel tubing into water was measured as a function of residence time of the water in the tubing as described in the experimental section. Some results are shown in Fig. 8. The dissolved total carbon dioxide in the tubing was found to be 2.8 and 7.6 μM for 9.5 and 60 min residence times respectively. Assuming the equilibrium sat-

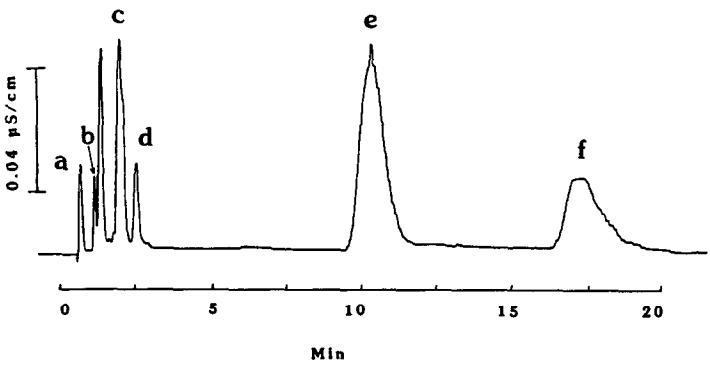

Fig. 7. Low level isocratic chromatogram obtained on the type 2 system. Eluent 39 mM NaOH. a = 1 μM F^-; b = 1 μM NO_2^-; c = 3.5 μM N_3^- + 5 μM SO_4^{2-}; d = 1 μM $C_2O_4^{2-}$; e = 20 μM PO_4^{3-}; and f = 12 μM I^-. The unmarked peak is from CO_2.

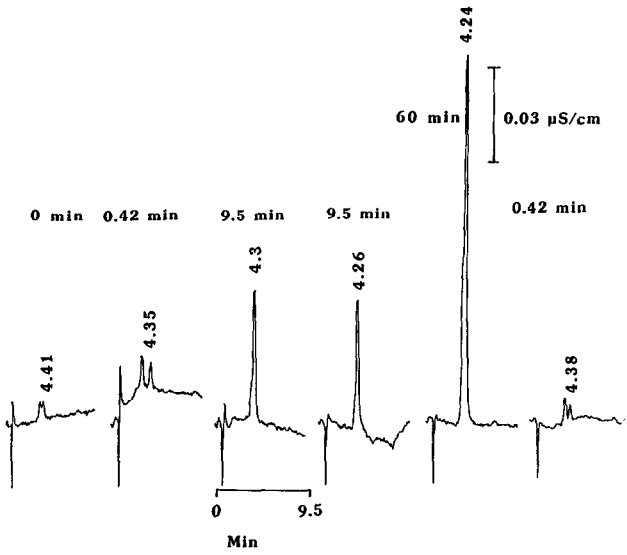

Fig. 8. Chromatograms illustrating the permeation of CO_2 through polymeric tubing with a wall thickness of 0.5 mm. Residence times are indicated.

uration value, C_s of carbon dioxide (aq.) to be 11 μM, the permeation rate of carbon dioxide through the tubing can be modelled as:

$$dC/dt = k(C_s - C') \quad (1)$$

where C', the undissociated carbon dioxide (aq.) in the tubing contents is related to the total dissolved carbon dioxide C, by:

$$C' = C - [-K + (K^2 + 4KC)^{0.5}]/2 \quad (2)$$

where K is the effective dissociation constant of "carbonic acid", $4.4 \cdot 10^{-7}$. Eqns. 1 and 2 were numerically evaluated to obtain the best fit value of the rate constant k to be $4.3 \cdot 10^{-4}$ s^{-1}. Considering that this pertains to a tube of 0.5 mm wall thickness and 0.5 mm internal diameter, the rate of carbon dioxide accumulation for short exposure times, *ca.* 0.3 μM/min, is remarkably large and emphasizes the need for the careful selection of the container and conduit material and minimizing residence times wherever possible if freedom from carbon dioxide contamination is to be maintained.

Strong acid anions —Response linearity and retention reproducibility. Linearity of response in suppressed IC at low concentrations is of considerable interest. This was determined for Cl^-, NO_3^- and SO_4^{2-} in the 0.03–100 μM concentration range. The linear coefficients of determination, r, were 0.998, 0.999 and 0.999, respectively. The slightly worse result for chloride indicates the difficulty of preparing this standard at low concentrations without contamination rather than any intrinsic non-linearity. The respective relative standard deviation of the slopes of the calibration lines were

1.4, 1.1 and 0.4%. The absolute retention times for the test ions are quite reproducible; mean absolute retention times (± S.D.) were: 2 (0.01), 6.01 (0.14) and 7.61 (0.06), respectively. The retention of nitrate is known to be partially controlled by hydrophobic interactions and as such is more susceptible to thermal effects; this is atypical.

Miscellaneous chromatographic applications. The excellent overall sensitivity of the system and facile gradient analysis led us to explore some unusual samples. Fig. 9 shows a series of gradient chromatograms. From bottom up, we progress through a system blank (which identifies the carbon dioxide still present in the system), an injection of water (residual chloride in this water is just visible), a dilute carbonate standard and the breath of a pipe smoker (one tidal volume exhaled through *ca.* 2 ml water). A comparison of these with a standard containing chloride and sulfate and a similar standard "spiked" with the exhaled air clearly shows that precursors to chloride and sulfate are present in the breath sample. The presence of metabolic hydrochloric acid is logical but whether the agent responsible for the sulfate peak is aerosol sulfate or gaseous sulfur dioxide is uncertain. At the levels involved, sulfite originally formed from dissolved sulfur dioxide is expected to be rapidly oxidized to sulfate, before or during chromatography.

Because the residual acidity in the EDG/EDS system is so low it seems likely that a variety of weak acid anions will give better conductometric response because of their greater dissociation at the detector compared to that in a carbonate or conventional sodium hydroxide system. This hypothesis was tested in a general way by

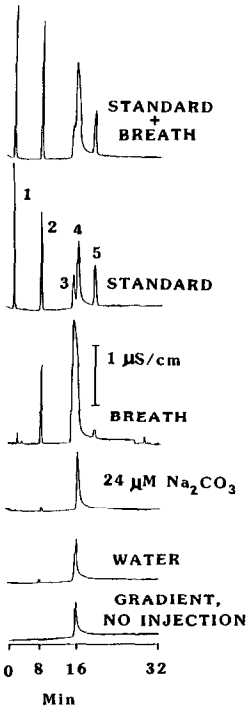

Fig. 9. Breath analysis. 1 = F^-; 2 = Cl^-; 3 = NO_3^-; and 4 = SO_4^{2-}; 30 μM each in the standard.

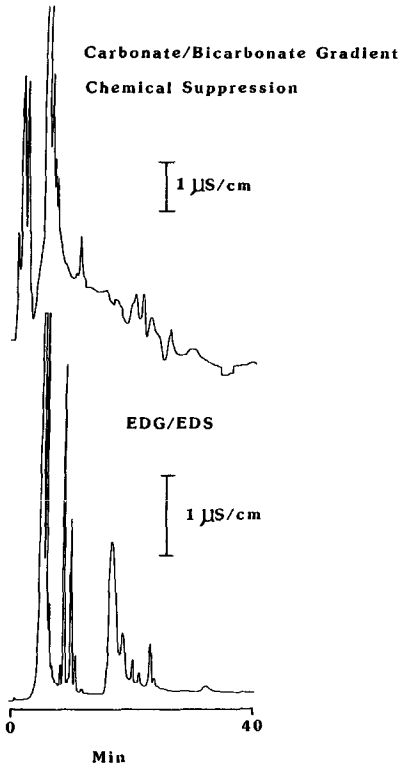

Fig. 10. Pipe smoke extract chromatograms. See text for details.

exhaling one tidal volume of pipe tobacco smoke through water as above and the resultant solution analyzed by IC, both with gradient EDG/EDS and gradient carbonate systems. The respective gradients were formulated to have very similar temporal elution strengths as judged by the retention times of the ions in a standard containing F^-, Cl^-, NO_3^- and SO_4^{2-}. Due to the considerable baseline rise involved in the carbonate gradient run, a blank baseline subtraction technique [24] was performed with this eluent. The results are shown in Fig. 10. Peaks eluting after *ca.* 15 min are difficult to demarcate in the carbonate run. These peaks are less numerous and of lower height even when the unsubtracted chromatogram is carefully examined, compared to the EDG/EDS run. The integrator identified 33% more peaks in the EDG/EDS run compared to the carbonate run.

CONCLUSION

An ultrapure sodium hydroxide generation system coupled with electrodialytic suppression affords an ion chromatographic system of unusual purity with respect to contamination by carbonate and ions derived from penetration of a chemical regenerant into the suppressed eluent. Freedom from carbonate results in much greater sensitivity for this ion while the general rejection of anions in the generator and lack

of acid regenerant bleed into the suppressed eluent (*ca.* 1.5 μM H^+ with 12.5 mM sulfuric acid) apparently allow for greater dissociation of and sensitivity for weak acids with pK_a values in the range 5–7.

The system was operated both in isocratic and gradient modes for several months. After stabilizing a new generator membrane by operating at various currents for *ca.* 3 h, the generated eluent concentration and resulting analyte retention times are repeatable on a day-to-day basis to better than *ca.* 3%. If the actual eluent concentration is conductometrically monitored, even better performance can be obtained.

ACKNOWLEDGEMENTS

We thank E. L. Loree (Bern Tech-Lite) for the design and fabrication of the flow-through thermostatic device, J. L. Lopez for the design, fabrication and programming of the programmable current generator and K. Friedman (Dionex) for helpful discussion. This research was supported by the US Department of Energy, through DE-FG05-84-ER13281 and by the Dionex Corporation. However, this manuscript was not subjected to review by the above agencies and no endorsements should be inferred. C.U.J. also thanks Soonchunhyang University for financial support.

REFERENCES

1 H. Small, *Ion Chromatography*, Plenum, New York, 1989, p. 170.
2 S. W. Downey and G. M. Hieftje, *Anal. Chim. Acta*, 153 (1983) 1.
3 L. J. Galante and G. M. Hieftje, *Anal. Chem.*, 59 (1987) 2293.
4 H. Shintani and P. K. Dasgupta, *Anal. Chem.*, 59 (1987) 1963.
5 L. J. Galante and G. M. Hieftje, *Anal. Chem.*, 60 (1988) 995.
6 T. Takeuchi, E. Suzuki and D. Ishii, *Chromatographia* 25 (1988) 582.
7 P. K. Dasgupta, *J. Chromatogr. Sci.*, 27 (1989) 422.
8 J. J. Conboy, D. J. Henion, M. W. Martin and J. A. Zweigenbaum, *Anal. Chem.*, 62 (1990) 800.
9 Y. Hanaoka, M. Takeshi, S. Muramoto, M. Tamizo and A. Nanba, *J. Chromatogr.*, 239 (1982) 537.
10 S. Rokushika, Z. L. Sun and H. Hatano, *J. Chromatogr.*, 253 (1982) 87.
11 S. Rokushika, Z. Y. Qiu and H. Hatano, *J. Chromatogr.*, 260 (1983) 81.
12 P. K. Dasgupta, R. Q. Bligh, V. D'Agostino and J. Lee, *Anal. Chem.*, 57 (1985) 253.
13 S. Gupta and P. K. Dasgupta, *J. Chromatogr. Sci.*, 26 (1988) 34.
14 T. Ban, T. Murayama, S. Muramoto and Y. Hanaoka, Yokagawa Electric Works, *U.S. Pat.*, 4 403 039 (1983).
15 K. H. Jansen, K. H. Fischer and B. Wolf, Biotronik Wissenschaftliche Geraete, *U.S. Pat.*, 4 459 357 (1984).
16 Z. W. Tian, R. Z. Hu, H. S. Lin and J. T. Wu, *J. Chromatogr.*, 439 (1988) 159.
17 D. L. Strong and P. K. Dasgupta, *Anal. Chem.*, 61 (1989) 939.
18 D. L. Strong, P. K. Dasgupta, K. Friedman and J. R. Stillian, *Anal. Chem.* 63 (1991) 480.
19 D. L. Strong and P. K. Dasgupta, *J. Membr. Sci.*, 57 (1991) 321.
20 J. R. Stillian, *LC Mag.*, 3 (1985) 802.
21 J. A. Dean (Editor), *Lange's Handbook of Chemistry*, McGraw-Hill, New York, 13th ed., 1969, pp. 6–42.
22 S. R. Palit, *Proc. 1st Australian Conference on Electrochemistry, Sydney 1963*, Hobart, Tasmania, 1965, p. 711.
23 K. Tanaka and J. S. Fritz, *Anal. Chem.*, 59 (1987) 708.
24. H. Shintani and P. K. Dasgupta, *Anal. Chem.*, 59 (1987) 802.